Available online at www.sciencedirect.com
SCIENCE DIRECT®
Journal of Chromatography A, 1092 (2005) 55–64
JOURNAL OF CHROMATOGRAPHY A
www.elsevier.com/locate/chroma

Enantioseparation of 1-phenyl-1-propanol by supercritical fluid-simulated moving bed chromatography

Arvind Rajendran[b], Stephanie Peper[a], Monika Johannsen[a], Marco Mazzotti[b,*], Massimo Morbidelli[c], Gerd Brunner[a]

[a] *Thermal Separation Processes, Technical University Hamburg-Harburg, Hamburg, Germany*
[b] *ETH Swiss Federal Institute of Technology Zurich, Institute of Process Engineering, ETH-Zentrum, ML G25, Sonneggstrasse 3, CH-8092 Zürich, Switzerland*
[c] *Institute for Chemical and Bioengineering (ICB), ETH Hönggerberg/HCI, CH-8093 Zürich, Switzerland*

Available online 8 March 2005

Abstract

The enantioseparation of 1-phenyl-1-propanol through the supercritical fluid-simulated moving bed (SF-SMB) process is studied. Non-linear isotherms were measured on an analytical column, and used together with the triangle theory for SMB design to select operating conditions for the SF-SMB. Experiments were carried out on a pilot-scale SF-SMB plant at conditions that corresponded to the non-linear range of the isotherm. Under conditions of low feed concentration, complete separation (extract purity = 99.5%; raffinate purity = 98.4%) was achieved. Under conditions of larger feed concentration, the best separation corresponded to an extract purity of 98.0% and a raffinate purity of 94.0%, and yielded a productivity of 110 g of racemate per kg stationary phase per day.

Keywords: Enantioseparation; Supercritical fluid-simulated moving bed chromatography; Triangle theory; Adsorption isotherm; 1-Phenyl-1-propanol

1. Introduction

The simulated moving bed (SMB) originally developed for petrochemical separations, finds extensive application in food and pharmaceutical industries [1,2]. In particular, separation of enantiomers where the separation factors are usually low, are being increasingly performed through SMB [3,4]. The SMB is an attempt to mimic the true moving bed (TMB) process shown in Fig. 1a. In the TMB, the solid phase is moved in a direction counter-current to that of the fluid phase, in which the solutes to be separated are fed continuously (between sections 2 and 3). The desorbent is fed continuously into section 1 and the products are collected at the extract and raffinate ports. The solvent that exits section 4 can then be recycled to section 1, whereas the solid phase is recycled from section 1 to section 4. If operated under suitable conditions, the solute mixture can be separated in a way that the weakly adsorbed solute (B) moves in the direction of the fluid and is collected at the raffinate port, while the strongly adsorbed solute (A) moves in the direction of the solid and is collected at the extract port. However, moving the solid causes practical difficulties and hence, the realization of a TMB is not easily achieved. The SMB, a schematic of which is shown in Fig. 1b, simulates the movement of the solid phase by simultaneously switching the inlet and exit ports periodically in the direction of fluid flow. The sections of the SMB have an analogous task as those in the TMB, i.e. sections 2 and 3 perform the separation of the solutes, while sections 1 and 4 are used to regenerate the stationary phase and the mobile phase, respectively.

Though the SMB has been chiefly operated in the liquid phase, gas phase processes have also been successfully demonstrated [5]. Clavier et al. [6] introduced also the concept of a supercritical fluid-simulated moving bed (SF-SMB), where a supercritical fluid, typically CO_2, is used as eluent. The use of supercritical CO_2 (sc-CO_2), leads to a number of advantages. Firstly, it reduces significantly the consumption of less benign organic solvents. Secondly, the physiochemical properties of supercritical fluid, e.g. viscosity and diffusivity, are favourable compared to liquids, thus leading to

* Corresponding author. Tel.: +41 44 632 2456/2486; fax: +41 44 632 1141.
E-mail address: marco.mazzotti@ipe.mavt.ethz.ch (M. Mazzotti).

0021-9673/$ – see front matter © 2005 Elsevier B.V. All rights reserved.
doi:10.1016/j.chroma.2005.02.040

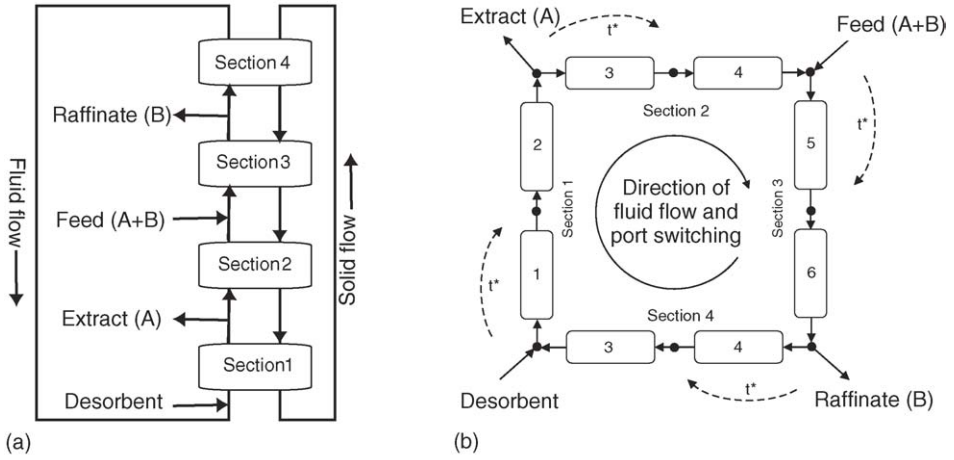

Fig. 1. Schematic of: (a) true moving bed (TMB); and (b) simulated moving bed (SMB). Components A and B are the strongly and weakly adsorbed solutes, respectively.

lower pressure drop and higher column efficiency. Thirdly, the retention behaviour of solutes in supercritical fluids shows a strong dependence on the mobile phase density and hence could be used to impose a gradient in the unit, thereby increasing the productivity of the process. As described before, each section of the SMB fulfills a specific task, and an advantage could be obtained by operating the unit in such a way that the solute is weakly retained in sections 1 and 2 and strongly retained in sections 3 and 4. This has been achieved, in liquid phase SMBs, by implementing a gradient of an intensive operating variable, e.g. temperature, solvent composition, etc. [7,8]. When a supercritical fluid is used as a mobile phase, the solute is strongly retained on the stationary phase at lower pressure owing to the lower solubility in the mobile phase, while it is weakly retained at higher pressures. Hence, by operating the unit under a pressure gradient mode, i.e. by maintaining section 1 at higher pressure and section 4 at a lower pressure, a gradient in elution strength over the SMB unit can be achieved. Realizing these advantages of using SF-SMB, studies have been performed and the operability of the process has been clearly demonstrated [9–11]. Further, it has been shown that operating the SF-SMB under pressure gradient mode can lead to an increase in productivity by a factor of 3.0 compared to the isocratic mode of operation [10].

The "triangle theory", based on the equilibrium theory of chromatography, offers simple design criteria for the operation of SMB units [12]. In its framework, the performance of the SMB unit is characterized by the ratio of the net flow of the mobile phase to that of the stationary phase, i.e. the m_j values, which are defined as:

$$m_j = \frac{Q_j t^* - V\epsilon}{V(1-\epsilon)} \quad (j = 1, \ldots, 4) \tag{1}$$

where Q_j is the volumetric flow rate in section j, t^* the switch time, and V and ϵ are the column volume and void fraction. In the case of liquids, the volumetric flow rate is constant over a section of the SMB. However, in the case of SF-SMB systems, the pressure drop along the section results in a gradient of the density, and hence the volumetric flow rate varies along a section itself. Under such conditions, the mass flow rate is the only parameter that is invariant and hence, for SF-SMB systems, Eq. (1) can be re-written in terms of the mass flow rate in section j, G_j, as:

$$m_j = \frac{G_j t^* - V\epsilon\rho_4}{V(1-\epsilon)} \tag{2}$$

where ρ_4 is the average density in section 4 [13]. Under conditions where the solute is present in dilute concentrations, the adsorption equilibrium can be represented by a linear isotherm:

$$n_i = H_i c_i \tag{3}$$

where n_i and c_i are the concentrations of component i in the solid and liquid phase, respectively, and H_i is the Henry constant. This equation can be written in terms of the weight fraction of component i in the mobile phase as:

$$n_i = H^*_{i,j} w_{i,j} \tag{4}$$

where

$$H^*_{i,j} = H_i \rho_j \tag{5}$$

and ρ_j is the density of the fluid phase in section j of the SF-SMB. Under these conditions, the necessary and sufficient conditions for complete separation in a SF-SMB unit are given by the following inequalities:

$$H^*_{\mathrm{A},1} < m_1 \tag{6a}$$

$$H^*_{\mathrm{B},2} < m_2 < H^*_{\mathrm{A},2} \tag{6b}$$

$$H^*_{\mathrm{B},3} < m_3 < H^*_{\mathrm{A},3} \tag{6c}$$

$$m_4 < H^*_{\mathrm{B},4} \tag{6d}$$

where A and B correspond, respectively, to the strongly and weakly adsorbed solutes. The inequalities corresponding to

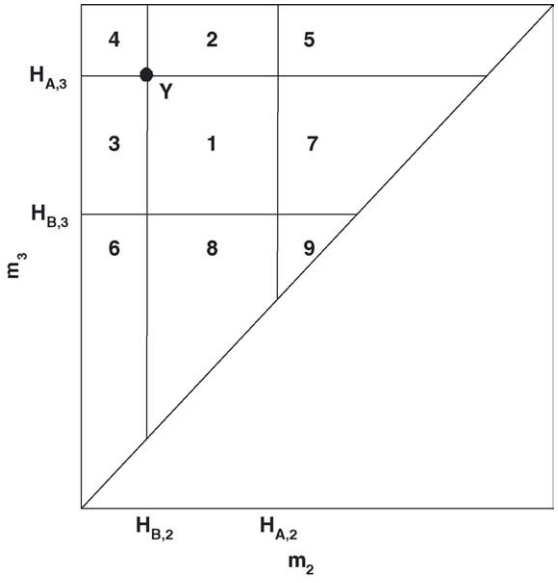

Fig. 2. Different separation regions of a SF-SMB operated under gradient mode. Region 1: complete separation region, $P_E = 100\%$, $P_R = 100\%$; region 2: $P_E = 100\%$, $P_R < 100\%$; region 3: $P_E < 100\%$, $P_R = 100\%$; region 4: $P_E < 100\%$, $P_R < 100\%$; region 5: extract flooded with the solvent while A and B are collected in the raffinate; region 6: raffinate flooded with the solvent while A and B are collected in the extract; region 7: extract flooded with pure solvent, B is collected in the raffinate, A accumulates in the unit; region 8: raffinate flooded with pure solvent, A is collected in the extract, B accumulates in the unit; region 9: both extract and raffinate flooded with pure solvent, both A and B accumulate in the unit. Y is the optimal operating point.

the sections 2 and 3, i.e. Eqs. (6b) and (6c) can be represented on the m_2–m_3 diagram for the generic case where $\rho_2 > \rho_3$ as shown in Fig. 2 and different operating regions can be identified. In a similar fashion, the regions of complete separation for the case of non-linear isotherms can be identified depending on the isotherm parameters and the concentration of the solutes in the feed [12]. The triangle theory, as mentioned before, is based on the equilibrium theory of chromatography in which mass transfer resistances are neglected, i.e. it is assumed that the efficiency of the columns is infinite. The efficiency of a column among other factors, depends on the diffusivity of the solutes in the mobile phase. Since the diffusivities of solutes in supercritical fluids are higher than those in liquids, the mass transfer resistance in SF-SMB is expected to be smaller than those in liquid-SMB, hence making the assumptions of the triangle theory more justifiable in SF-SMB design than in the case of liquid-SMBs (HPLC-SMB). Moreover, the validity of the triangle theory for SF-SMB design has been tested by experimental results [9–11].

The separation of the enantiomers of 1-phenyl-1-propanol, which is the objective of this work, has already been carried out on HPLC-SMB using Chiralcel-OB as a stationary phase [14]. A productivity of 11.69 g per kg stationary phase per day was reported with the purities of the extract and raffinate fractions being 95.4% and 98.5%, respectively. The solvent consumption was 1.21 L/g of racemate separated.

In this work, the enantioseparation of 1-phenyl-1-propanol by SF-SMB is studied. The measurement of non-linear adsorption isotherm parameters at analytical scale and the subsequent implementation of the separation on a pilot scale SF-SMB unit is described. The results from these experiments shall be discussed in light of the triangle theory for SF-SMB design.

2. Determination of non-linear adsorption isotherms

2.1. Materials

Racemic mixture (97.4% purity), pure enantiomers *R* and *S* (99.0% purity) of 1-phenyl-1-propanol and HPLC grade methanol (99.8% purity) were obtained from Fluka Chemie, Buchs, Switzerland. Carbon dioxide (99.995% purity) was obtained from PanGas AG, Luzern, Switzerland. A commercially packed 250 mm long, 4 mm diameter Chiralcel-OD column with 20 μm particle size from Chiral Technologies Europe, Illkrich-Cedex, France, was used for the characterization experiments.

2.2. Experimental procedure

The experimental set-up consists of syringe pumps to deliver constant flow rates of CO_2 and modifier to the column which is housed in a thermostatted water bath maintained at 30 °C. A pulse of the test solute is injected using a motor activated valve and the chromatographic response is measured using a UV detector. A back pressure regulator located downstream of the UV detector maintains the pressure in the system. The details of the set-up are given elsewhere [15].

The solute 1-phenyl-1-propanol was diluted in MeOH to prepare solutions for the pulse injection. Solutions of the pure enantiomers with a concentration of 200.0 g/L of pure enantiomer were prepared to determine the adsorption isotherms, while solutions of the racemate with concentrations 63.7, 98.3 and 244.0 g/L of racemate were prepared to study the effect of competitive adsorption. The CO_2 pump, the head of which was maintained at 15 °C, was set to a constant flow rate of 1 mL/min and the modifier pump was set to a suitable flow rate to produce the desired modifier concentration in the mobile phase. Once hydrodynamic steady state was reached, a pulse of the solute was injected through the valve which had an external sample loop of 20.5 μL. Independent injections of the solutions of pure enantiomers and of the racemate were made. The UV responses (measured at $\lambda = 259$ nm) to the injections of the pure component and the racemate were used to obtain the calibration of the UV detector while the response to the injection of the pure enantiomers were used for the determination of the isotherm parameters.

The concentration of component *i* in the fluid phase, c_i, is proportional to the UV signal, *S*:

$$c_i = \alpha_i S \tag{7}$$

In the present case, both enantiomers exhibit the same UV absorbance characteristics, hence the value of α_i is identical for both. Since the UV absorbance of the solute also depends on the solvent composition and the operating pressure, α_i depends on the operating conditions and therefore has to be evaluated independently whenever these change. For a particular operating condition, the value of α_i was estimated by minimizing the sum of the squared errors, J:

$$J = \sum_{k=1}^{k=5} \left(c_k^{\text{pulse}} V_k^{\text{loop}} - Q \int_{t_k^{\text{start}}}^{t_k^{\text{end}}} \alpha_i S(t)\, \mathrm{d}t \right)^2 \quad (8)$$

where k corresponds to the injection number. For each experimental condition, five injections were performed, namely two for the pure enantiomers and three for the racemates. In the above equation, c^{pulse} is the concentration of the injected solution, V^{loop} the volume of the sample loop, Q the volumetric flow rate and t^{start} and t^{end} are the times at which the 1-phenyl-1-propanol peak starts and ends, respectively. The first term in the summation in Eq. (8) is the total mass injected, while the second corresponds to the mass of solute obtained by integrating the chromatographic response, i.e. the amount collected at the column outlet. From the minimization of J in Eq. (8), the value of α_i was determined, which was then used to transform the UV signal into concentration units.

The responses to the pulse injections of the pure enantiomer solutions at 17 MPa and 2.7% (w/w) of modifier concentration are shown in Fig. 3. Based on the shape of the pulse responses, a competitive Langmuir model was chosen to represent the adsorption equilibria:

$$n_i = \frac{H_i c_i}{1 + k_R c_R + k_S c_S} \quad (i = R, S) \quad (9)$$

where the Henry constant, H_i, is expressed as:

$$H_i = \Gamma_i k_i \quad (i = R, S) \quad (10)$$

with Γ_i and k_i being, respectively, the saturation capacity and the equilibrium constant of component i. In the present study, it was assumed that the mobile phase constituents namely MeOH and CO_2, do not compete for adsorption sites and hence the isotherm equation represented by Eq. (9) accounts only for the competition between the enantiomers R and S. In an earlier study, H_i has been obtained as a function of mobile phase density and modifier concentration for both the enantiomers, by injecting low concentration pulses [15]. Hence, for each enantiomer, of the two parameters, Γ_i and k_i, only one needs to be estimated to describe the non-linear adsorption isotherm of Eq. (9). The Langmuir isotherm parameters, k_R, k_S, Γ_R, Γ_S, of the two enantiomers, were fitted independently to the pulse response of the pure enantiomers with the constraint that the Henry constant values be equal to those estimated earlier. The values of k_i and Γ_i for two different modifier concentrations, 2.5% (w/w) and 2.7% (w/w) are given in Table 1 and the corresponding pure component isotherms at $P = 17.0$ MPa, $c_m = 2.7\%$ (w/w) are shown in Fig. 4.

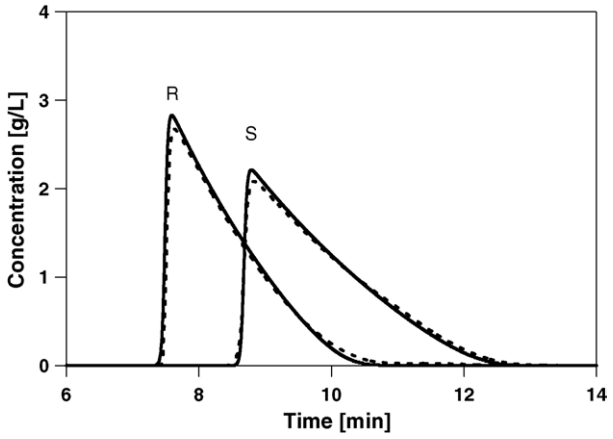

Fig. 3. Experimental (dotted line) and simulated (solid line) pulse responses of injections of pure enantiomers of 1-phenyl-1-propanol. Conditions: pressure, 17.0 MPa; temperature, 30 °C; modifier concentration, 2.7% (w/w); concentration of pulse, *R* enantiomer 195.94 g/L, *S* enantiomer 198.98 g/L.

A column model based on the linear driving force description of mass transfer was used to simulate the pulse response of the pure enantiomers. The mass transfer and axial dispersion parameters were chosen in order to fit the chromatograms. The comparison of the experimental pulse response and the simulation is illustrated in Fig. 3. The simulation captures the experimental response well. In order to test the suitability of the competitive Langmuir isotherm to describe injections of binary mixtures, the column model was used to predict the pulse responses to racemic injections. The comparison between experimental data and simulation results at $P = 17.0$ MPa, $c_m = 2.7\%$, and $c^{\text{pulse}} = 244$ g racemate/L is illustrated in Fig. 5 showing a reasonably good agreement. The experimental response exhibits, however, a peculiar peak distortion in the range between 9 and 10 min, i.e. a behaviour that was not observed in the experiments at lower pulse concentration. However, the fronts in general are well described by the model up to the concentrations studied here, hence the pure component parameters can be used to identify operating regions for the SMB separation.

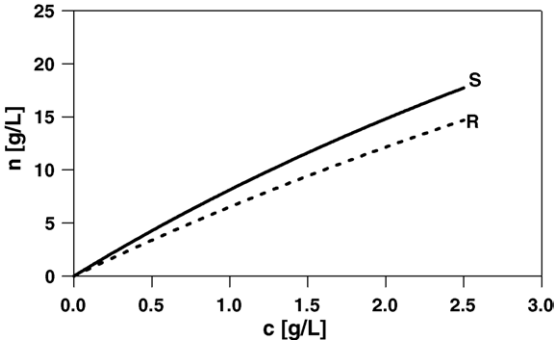

Fig. 4. Measured non-linear isotherms at $P = 17.0$ MPa, $c_m = 2.7\%$ (w/w) of the enantiomers of 1-phenyl-1-propanol at 30 °C.

Table 1
Non-linear adsorption isotherm parameters of 1-phenyl-1-propanol on Chiralcel-OD at selected operating conditions

Pressure (MPa)	$c_m = 2.7\%$ (w/w)				$c_m = 2.5\%$ (w/w)			
	Γ_R (g/L)	k_R (L/g)	Γ_S (g/L)	k_S (L/g)	Γ_R (g/L)	k_R (L/g)	Γ_R (g/L)	k_S (L/g)
17.0	89.33	0.079	83.44	0.108	90.39	0.082	81.21	0.116
15.5	78.91	0.095	70.47	0.136	83.27	0.094	78.36	0.128

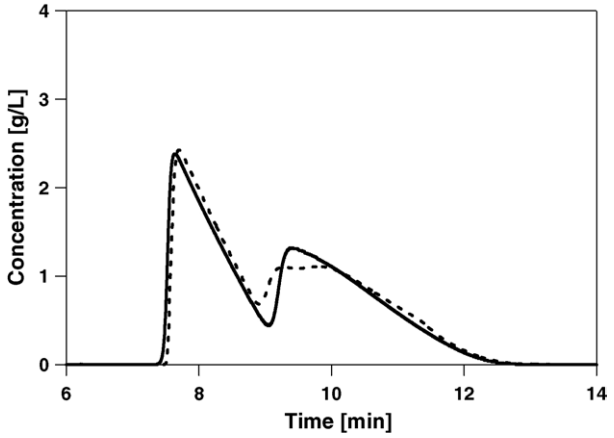

Fig. 5. Experimental (dotted line) and simulated (solid line) pulse responses of injections of racemic mixture of the enantiomers of 1-phenyl-1-propanol. Conditions: pressure, 17.0 MPa; temperature, 30 °C; modifier concentration, 2.7% (w/w); concentration of pulse, 244.31 g racemate/L.

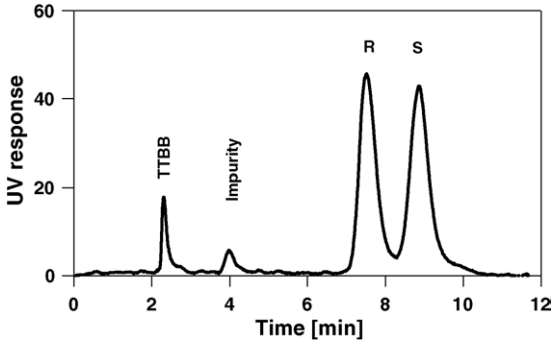

Fig. 6. Response of the preparative self-packed column (column 7) to a pulse of the racemic mixture of 1-phenyl-1-propanol. Operating conditions: pressure, 18.0 MPa; $c_m = 2.55\%$ (w/w); flow rate, 30 g/min.

3. SF-SMB separation

3.1. Materials

Carbon dioxide (purity >99.95%) for the SF-SMB experiments was obtained from Bad Hönningen, Germany. Methanol (purity >99.95%) and isopropanol (purity >99.95%) were obtained from Merck, Darmstadt, Germany. Racemic mixture of 1-phenyl-1-propanol (purity >98.4%) was obtained from Fluka Chemie, Sigma–Aldrich Chemie, Munich, Germany. The stationary phase, Chiralcel-OD, with an average particle size of 20 μm obtained from Daicel Europe, was loaned from Carbogen AG, Aarau, Switzerland.

3.2. Column packing and characterization

A slurry prepared by mixing about 55 g of Chiralcel-OD (average particle diameter 20 μm) with 110 mL of isopropanol (IPA) was poured into the column and IPA was partially removed by applying vacuum. The piston of the dynamic axial compression (DAC) unit was mounted and a pressure of 5.5 MPa was applied, thus removing a part of the IPA and compressing the bed. The residual IPA was withdrawn by letting CO_2 flow through the unit, and then each column was tested to measure the porosity and to evaluate the quality of the packing. A mobile phase consisting of CO_2 and MeOH (2.55%, w/w) at a pressure of 18.0 MPa was pumped at a flow rate of 30 g/min. A pulse of diluted racemic mixture of 1-phenyl-1-propanol with a small amount of 1,3,5-tri-*tert*-butyl-benzene (TTBB) in MeOH was injected and the response was measured using a UV detector. A sample chromatogram from column 7 is shown in Fig. 6. A clear separation of the peaks was observed in all the columns. The average number of plates per column was 1500, thus indicating that the packing quality was good. Since in the previous study [15] it was shown that the TTBB can exhibit retention on the stationary phase, the column porosities were obtained by fitting the retention times obtained in the characterization injections to those calculated by using the Henry constants from analytical injections. The average value of ϵ was 0.732 ± 0.013.

3.3. Description and operation of the SF-SMB unit

The separation was performed on the SF-SMB pilot unit at the Technische Universität Hamburg-Harburg. A brief description of the unit, shown in Fig. 7, is given here, while more details are given elsewhere [9]. The unit, based on the purported task, can be divided into three sub-units: (1) feed; (2) columns and switch valves; and (3) cyclones for product separation. The feeding system provides a continuous supply of the eluent and the feed to the unit. The CO_2 from the storage was liquefied by cooling and then pumped to a required pressure level using an air driven pump. The pressurized CO_2 was split into two streams, one each for the desorbent and the feed. The CO_2 at the desired pressure was then mixed with the MeOH which was pumped continuously using a HPLC pump. The mixture was brought to the desired operating temperature and fed to the desorbent switch valve. The feed CO_2 stream, the pressure of which was independently regulated, was mixed with the solute (a racemic mixture of 1-phenyl-1-propanol dissolved in MeOH) and pumped using a HPLC pump. The feed flow rate was metered and regulated manually

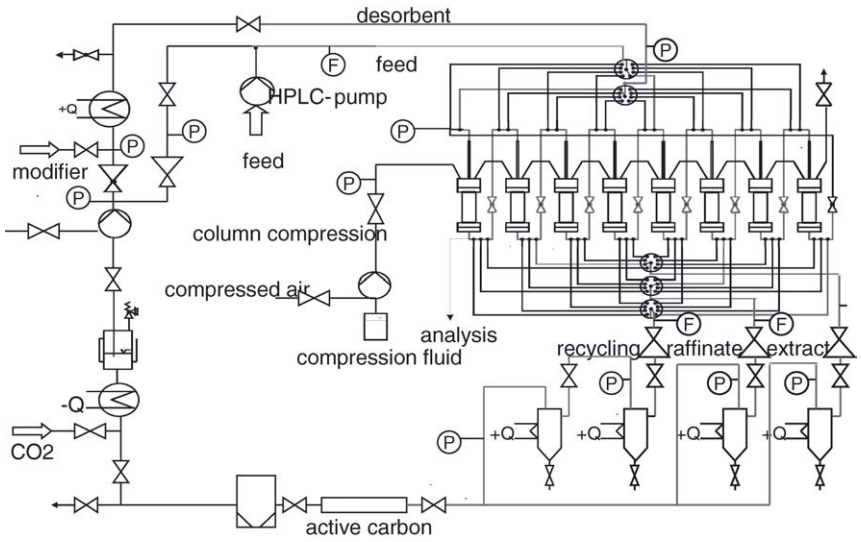

Fig. 7. Schematic of the SF-SMB plant used in the study.

using a fine-regulation valve. The core of the plant consisted of eight electrically thermostatted columns, each of 3 cm diameter, and 8 + 1 port switching valves, i.e. one valve each for the desorbent, extract, feed, raffinate and the recycle. A pressure sensor was located in between columns 7 and 8, while a 100 μL loop was located between columns 1 and 2 to measure the internal concentration profile in the unit by sampling and off-line analysis. The columns were equipped with a dynamic axial compression unit. In the present study, MeOH was used as compression fluid and the pressure in the axial compression unit was maintained 1.0–2.0 MPa above the maximum fluid pressure in the SF-SMB unit. The extract, raffinate and recycle flows were monitored and controlled manually by metering valves located upstream of the cyclones. The cyclones were maintained at about 5.0 MPa and were heated to provide conditions that cause the separation of the modifier and the solute from the CO_2 phase. The CO_2 leaving the cyclones was vented; the SF-SMB unit was run therefore in an open-loop 2-2-2-2 configuration, i.e. with two columns in each section. The operating temperature was 30 °C.

After start-up, once hydrodynamic steady state was reached, i.e. with pressure and flow rates at a steady value, the feed was introduced and the internal concentration profile was monitored. When the unit reached cyclic steady state, sample collection was started; the operation was then continued for about 8–10 cycles. The feed, extract and recycle purities were analyzed off-line using a Hewlett-Packard SFC system, with Chiralcel-OB as stationary phase and CO_2 + IPA as mobile phase.

3.4. Experimental results

Three sets of experiments grouped according to the feed concentration were performed (see Table 2). The experiments of groups A and B correspond to feed concentrations of 0.34 and 7.02 mg of racemate/g of feed, respectively. Within each group, the values of the external flow rates, namely those of the desorbent, extract, feed, raffinate, and recycle, were maintained constant, whereas the switch time was varied. The region of complete separation in the (m_2, m_3) plane, based on the triangle theory, for the experimental runs under group A is shown in Fig. 8a. It is worth noting that in these experiments the average modifier concentration in sections 1 and 2 was 2.69% (w/w), while in sections 3 and 4 it was 2.54% (w/w). The modifier gradient offers a minor improvement to the separation performance of the system and leads to the existence of a feasibility boundary in the (m_2, m_3) plane (shown as a dotted line) separating the accessible area (above the line) from the inaccessible one (below the line) for operation [8]. In the present study, since the Henry constants of the solutes are high, the time it takes after a switch for the equilibration of the column with new modifier concentration would be much shorter than the switch time. Hence,

Table 2
Classification of experiments according to operating conditions

Group	c_F (mg racemate/g feed)	V (mL)	P_1 (MPa)	P_2 (MPa)	P_3 (MPa)	P_4 (MPa)	$c_{m,1\text{ and }2}$ (%, w/w)	$c_{m,3\text{ and }4}$ (%, w/w)
A	0.34	99.14	17.1	16.7	16.4	16.1	2.69	2.54
B	7.02	98.72	17.2	16.8	16.5	16.2	2.69	2.54
C	3.54	91.18	16.8	15.9	14.5	13.8	2.68	2.68

The values reported correspond to the arithmetic average of all the runs performed under one group.

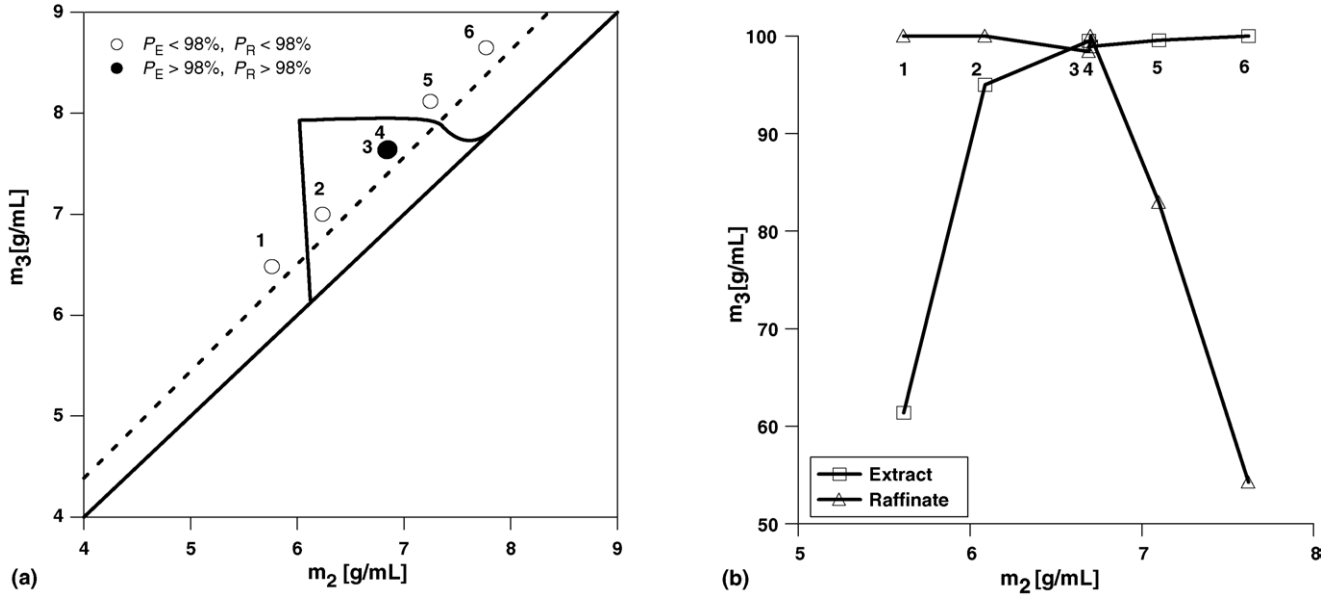

Fig. 8. Results of experimental runs in group A. (a) Comparison of operating points of experimental runs (symbols) with complete separation region calculated using the triangle theory. (b) Extract and raffinate purities of experimental runs as a function of m_2. Points correspond to experimental measurements, while lines are drawn to guide the eye.

it can be safely assumed that the separation conditions can be calculated using the isotherm parameters corresponding to the final composition of the mobile phase. Following such a reasoning, the boundaries of the complete separation region have been calculated by using the average values of the pressures and modifier concentration in each section as in the previous work [8]. For conditions at which the isotherm parameters were not directly measured, the value of Γ_i at a particular pressure was interpolated from the data obtained at two bracketing pressure values (see Table 1) and the equilibrium constant, k_i, was obtained from this and the Henry coefficient that was measured independently.

The experimental m_j values were calculated using Eq. (2) which is applicable to the situation where no extra-column dead volume exists in the unit. However, in a situation where there are dead volumes, a suitable correction has to be applied [16]:

$$m_j = \frac{G_j t^* - V\epsilon\rho_4}{V(1-\epsilon)} - \frac{V_d\rho_4}{V(1-\epsilon)} \tag{11}$$

where V_d is the dead volume per column, which in the present study was 4.82 mL. The parameters needed to calculate the m_j values are the mass flow rates in section j, G_j, the volume of the column, V, and its porosity, ϵ. The mass flow rates were obtained from the readings of the mass flow meters at hydrodynamic steady state, while the volume of the column, V, was calculated from the piston position of the DAC unit in each column. Among the different columns in the unit, there were minor variations in the column volume, and for the calculation of the m_j an average value of V as given in Table 2 was used. The value of $\epsilon = 0.719$ has been used for all the experiments in groups A and B.

Table 3
Operating conditions of the experimental runs reported

Group	Run no.	t^* (s)	m_1 (g/mL)	m_2 (g/mL)	m_3 (g/mL)	m_4 (g/mL)	P_E (%)	P_R(%)
A	1	240	8.50	5.76	6.48	2.00	61.4	100.0
	2	255	9.15	6.24	7.00	2.27	95.0	100.0
	3	270	9.93	6.84	7.63	2.54	99.5	98.4
	4	270	9.94	6.85	7.64	2.54	98.9	100.0
	5	285	10.50	7.25	8.12	2.81	99.6	83.0
	6	300	11.22	7.77	8.65	3.09	100.0	54.3
B	7	210	7.22	4.79	5.37	1.46	84.9	95.4
	8	225	7.86	5.28	5.93	1.74	98.0	94.1
	9	240	8.56	5.81	6.53	2.12	100.0	75.1
	10	270	9.88	6.78	7.59	2.56	99.2	57.1
C	11	240	8.70	5.77	6.46	2.31	89.7	100.0
	12	245	9.00	6.01	6.71	2.36	96.2	100.0
	13	245	9.04	6.06	6.73	2.39	98.2	100.0
	14	260	9.70	6.53	7.26	2.65	100.0	75.4

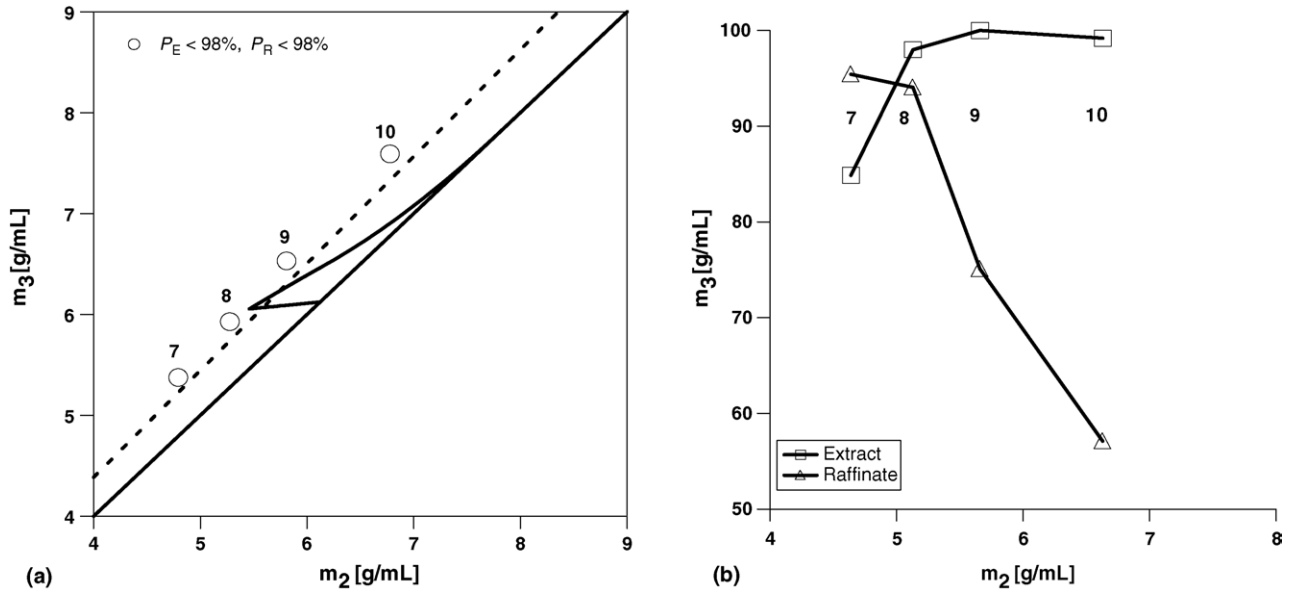

Fig. 9. Results of experimental runs in group B. (a) Comparison of operating points of experimental runs (symbols) with complete separation region calculated using the triangle theory. (b) Extract and raffinate purities of experimental runs as a function of m_2. Points correspond to experimental measurements, while lines are drawn to guide the eye.

The operating conditions of the experimental runs and the corresponding purities of the extract and raffinate streams are given in Table 3. The operating points of experimental runs in group A are plotted together with the complete separation region in the (m_2, m_3) plane calculated using the triangle theory in Fig. 8a, while Fig. 8b shows the experimental purities as a function of m_2. The corresponding plots for the runs in group B are shown in Figs. 9a and b, respectively. From Fig. 8a, it can be seen that the experiments span different operating regions with runs 2–4 being within the complete separation region. However, in the case of group B in Fig. 9a, it can be noticed that most of the complete separation region lies below the feasibility boundary, thus making it hardly accessible. This reflects the limited loadability of the stationary phase under the present operating conditions. The vertex of the triangle is, however, just above the boundary, hence operating the SF-SMB in its vicinity will provide the best achievable separation. This is evidenced by the experimental purities corresponding to run 8, whose m_j values are nearest to the vertex. This run resulted in $P_E = 98.0\%$ and $P_R = 94.1\%$. These results correspond to a productivity of 110 g of racemate per kg stationary phase per day, a solvent consumption of 2.3 kg CO_2/g racemate, and a MeOH consumption of 0.082 L/g racemate. The purities of extract and raffinate, as it can be seen in Figs. 8b and 9b, exhibit the expected trends, i.e. increasing the value of m_2 moves the unit operation from pure raffinate conditions to pure extract conditions, passing through a region where both raffinate and extract were obtained with high purities. It can be noticed that in the case of group A, two runs, namely runs 3 and 4, achieved complete separation, contrary to group B for the reasons mentioned above. Runs 3 and 4, which were two independent runs but with the same operating parameters, demonstrate that the results obtained are indeed reproducible. Run 2 is the only experiment which does not quantitatively match the predictions of the triangle theory.

Using the injection loops located between columns 1 and 2, it was possible to obtain the concentration profile in the system. The steady-state concentration profile corresponding to run 3 is shown in Fig. 10. The figure clearly shows the establishment of the familiar steady state SMB concentration profile that would yield the complete separation of the enantiomers.

Experiments in group C were run after a set of experiments performed at high flow rate conditions and large pressure drop (17.0 MPa) across the unit. These led to an increase of the DAC pressure up to 28.0 MPa. These were conditions where

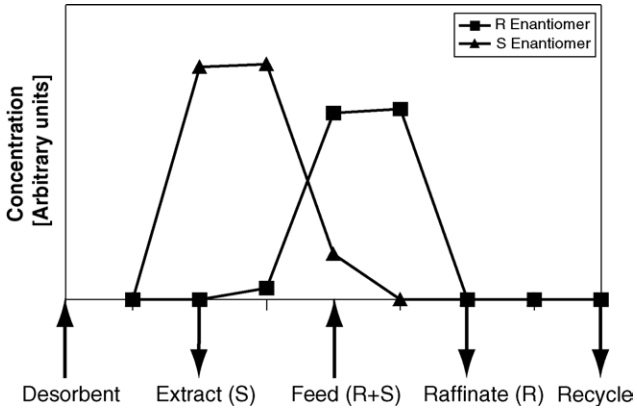

Fig. 10. Concentration profile in the SF-SMB under cyclic steady state conditions. The concentration measurements were performed using the sample loop located between columns 1 and 2, 20 s after the switch. Points correspond to experimental measurements, while lines are drawn to guide the eye.

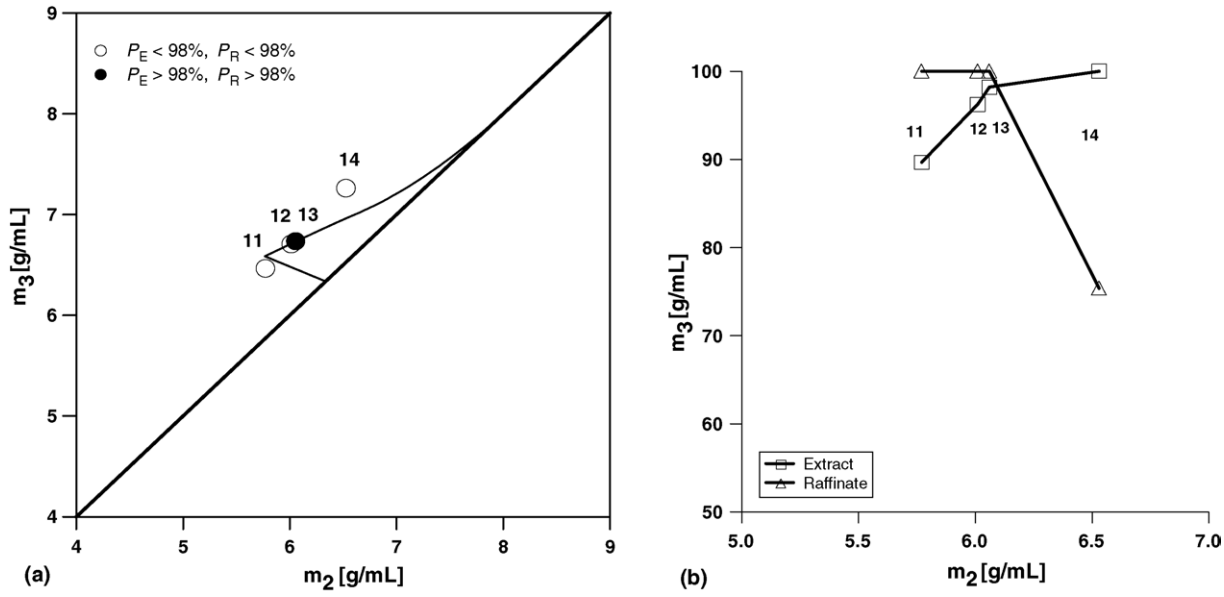

Fig. 11. Results of experimental runs in group C. (a) Comparison of operating points of experimental runs (symbols) with complete separation region calculated using the triangle theory. (b) Extract and raffinate purities of experimental runs as a function of m_2. Points correspond to experimental measurements, while lines are drawn to guide the eye.

the pressure difference between the fluid in the column and that in the DAC unit was as high as 21.5 MPa. This caused further compression of the beds which resulted in a reduction of the average column volume by 8% (see Table 2). It can also be seen that the pressure drops observed in the unit in the group of experiments were larger than those in groups A and B, despite the similar flow rates. The change in the volume of the bed indicates that there would be a change in the bed void fraction. Assuming that there is no loss of solid, and that the change in void fraction occurs through compression of the stationary phase, the following relationship can be written:

$$V_C(1-\epsilon_C) = V_{A,B}(1-\epsilon_{A,B}) \tag{12}$$

where the subscripts refer to the conditions in the different groups of experiments. Eq. (12) yields (using data in Table 2):

$$\epsilon_C = 1-(1-\epsilon_{A,B})\frac{V_{A,B}}{V_C} = 0.69 \tag{13}$$

The complete separation region for the experiments in group C is shown in Fig. 11a. The experimental m_j values were calculated using ϵ_C and are represented as symbols in the (m_2, m_3) plane in Fig. 11a. The dependence of the purities on m_2 is shown in Fig. 11b. It can be seen that complete separation was achieved in run 13. Run 12 was performed with the same switch time as that of run 13, but with slightly different flow rates. This resulted in the m_j values of run 13 being slightly smaller than those of run 12. The operating point of run 13 lies on the border of the triangle and exhibits complete separation, while run 12 yielded slightly lower purity of the extract. These points are close to the vertex of the triangle and slight disturbances in terms of flow rates can cause differences in the purities, since in the neighbourhood of the vertex, the separation performance is most sensitive to changes in operating conditions. However, as seen from Fig. 11b, the trends of the purities when plotted as a function of m_2 are similar to those in groups A and B, and conform to the expected behaviour.

4. Conclusion

The separation of the enantiomers of 1-phenyl-1-propanol on Chiralcel-OD by SF-SMB has been studied. The isotherms under non-linear regimes were measured on an analytical column. These results were used to identify regions of complete separation for the SF-SMB operation. Complete separation was achieved at low feed concentrations. At higher value of the feed concentration, the best separation achieved yielded $P_E = 98\%$ and $P_R = 94\%$. The productivity obtained was 110 g of racemate per kg stationary phase per day. The productivity is limited owing to a lower loadability of the stationary phase. However, the solvent consumption was 0.082 L MeOH/g racemate, which is substantially lower than in HPLC-SMB systems. It was further demonstrated that the triangle theory is well suited for the design of SF-SMB units.

5. Nomenclature

c	fluid phase concentration of solute (g/L)
G	mass flow rate (g/s)
H	Henry constant
H^*	modified Henry constant (g/mL)

k	equilibrium constant in Langmuir isotherm (L/g)
m	flow rate ratio (g/mL)
n	solid phase concentration of solute (g/L)
P	purity (%)
Q	volumetric flow rate (mL/s)
S	UV signal (ABU)
t^*	switch time (s)
V	column volume (mL)
V_{loop}	volume of injection loop (mL)
w	weight fraction of solute in the fluid phase (g of solute/g of mobile phase)

Greek letters

α	UV calibration parameter (g/(L ABU))
Γ	saturation capacity of the solid (g/L)
ϵ	column void fraction
ρ	density (g/mL)

Subscripts and superscripts

d	dead volume
D	desorbent
E	extract
F	feed
i	component
j	section of SMB
m	modifier
R	raffinate

Acknowledgements

The loan of stationary phase from Dr. Markus Juza, Carbogen AG, Aarau, Switzerland and the financial support from the Swiss National Science Foundation (SNF) through grant SNF 20-6798902 are gratefully acknowledged.

References

[1] D.M. Ruthven, C.B. Ching, Chem. Eng. Sci. 44 (1989) 1011.
[2] M. Juza, M. Mazzotti, M. Morbidelli, Trends Biotechnol. 18 (2000) 108.
[3] M. Schulte, J. Strube, J. Chromatogr. A 906 (2001) 399.
[4] J.E. Rekoske, AIChE J. 47 (2001) 2.
[5] M. Juza, O. Di Giovanni, G. Biressi, V. Schurig, M. Mazzotti, M. Morbidelli, J. Chromatogr. A 813 (1998) 333.
[6] J.Y. Clavier, R.M. Nicoud, M. Perrut, in: Ph.R. von Rohr, Ch. Trepp (Eds.), High Pressure Chemical Engineering, Elsevier, 1996.
[7] C. Migliorini, M. Wendlinger, M. Mazzotti, M. Morbidelli, Ind. Eng. Chem. Res. 40 (2001) 2606.
[8] S. Abel, M. Mazzotti, M. Morbidelli, J. Chromatogr. A 944 (2002) 23.
[9] A. Depta, T. Giese, M. Johannsen, G. Brunner, J. Chromatogr. A 865 (1999) 175.
[10] F. Denet, W. Hauck, R.M. Nicoud, O. Di Giovanni, M. Mazzotti, J.N. Jaubert, M. Morbidelli, Ind. Eng. Chem. Res. 40 (2001) 4603.
[11] S. Peper, M. Lübbert, M. Johannsen, G. Brunner, Sep. Sci. Technol. 37 (2002) 2545.
[12] M. Mazzotti, G. Storti, M. Morbidelli, J. Chromatogr. A 769 (1997) 3.
[13] O. Di Giovanni, M. Mazzotti, M. Morbidelli, F. Denet, W. Hauck, R.M. Nicoud, J. Chromatogr. A 919 (2001) 1.
[14] S. Khattabi, D.E. Cherrak, K. Mihlbachler, G. Guiochon, J. Chromatogr. A 893 (2000) 307.
[15] A. Rajendran, M. Mazzotti, M. Morbidelli, J. Chromatogr. A, submitted for publication.
[16] C. Migliorini, M. Mazzotti, M. Morbidelli, AIChE J. 45 (1999) 1411.